

Electronic Supplementary Information for

## Highly efficient and selective aqueous phase hydrogenolysis of furfural to 1,5-pentanediol using bimetallic Ru-SnO<sub>x</sub>/γ-Al<sub>2</sub>O<sub>3</sub> catalysts†

Rodiansono,<sup>\*a,b,c</sup> Atina Sabila Azzahra,<sup>b</sup> Uripto Trisno Santoso,<sup>a,b</sup> Edi Mikrianto,<sup>a,b</sup> Eka Suarso,<sup>c</sup> Kiky Corneliasari Sembiring,<sup>d</sup> Indri Badria Adilina,<sup>d</sup> Gagus Ketut Sunnardianto,<sup>e</sup> Ahmad Afandi<sup>f</sup>

---

<sup>a</sup> Department of Chemistry, Lambung Mangkurat University, Jl. A. Yani Km 36 Banjarbaru, Indonesia 70714.  
Telp. / Fax: +62 511 477 3112.

<sup>b</sup> Inorganic Materials & Catalysis (IMCat), Catalysis for Sustainable Energy & Environment (CATSuRe),  
Lambung Mangkurat University.

<sup>c</sup> Department of Physics, Lambung Mangkurat University, Jl. A. Yani Km 36 Banjarbaru, Indonesia.

<sup>d</sup> Research Centre for Advanced Chemistry, BRIN, Puspiptek Serpong, Tangerang.

<sup>e</sup> Research Centre for Quantum Physics, BRIN, Puspiptek Serpong, Tangerang.

<sup>f</sup> Research Centre for Advanced Materials, BRIN, KST BJ Habibie Serpong, Tangerang.

---

Corresponding authors: [rodiansono@ulm.ac.id](mailto:rodiansono@ulm.ac.id) (R. Rodiansono). Tel./fax: +62 511 477 3112

### Contents:

- 1) XRD patterns of the hydrargillite-derived γ-Al<sub>2</sub>O<sub>3</sub>-500, and three types commercially available of Cariact-γ-Al<sub>2</sub>O<sub>3</sub>(E) (Evonik); (γ-Al<sub>2</sub>O<sub>3</sub>(H) (HWNANO), and -γ-Al<sub>2</sub>O<sub>3</sub>(M) (Merck) (**Fig. S1**).
- 2) XRD patterns of unreduced (as-prepared) and reduced Ru-(1.30)Sn/γ-Al<sub>2</sub>O<sub>3</sub>(E) samples (**Fig. S2**).
- 3) (a) N<sub>2</sub>-adsorption-desorption profiles and (b) pore sizes distribution determined by DFT method for four types of gamma-alumina-based supported Ru-(1.30)Sn catalysts after reduction with H<sub>2</sub> at 400 °C for 2 h (**Fig. S3**).
- 4) NH<sub>3</sub>-TPD profiles of Ru-(x)Sn/γ-Al<sub>2</sub>O<sub>3</sub>(E) and deconvoluted NH<sub>3</sub>-TPD spectra of Ru-(0.65)Sn/γ-Al<sub>2</sub>O<sub>3</sub>(E), Ru-(1.30)Sn/γ-Al<sub>2</sub>O<sub>3</sub>(E), and Ru-(2.15)Sn/γ-Al<sub>2</sub>O<sub>3</sub>(E) catalysts (**Fig. S4**).
- 5) XPS spectra Al 2p for fresh and spent Ru-(1.30)Sn/g-Al<sub>2</sub>O<sub>3</sub>(E) samples (**Fig. S5**).
- 6) GC chart (chromatogram) of reaction mixture obtained from the reaction of FFald in 1,4-dioxane using the most effective Ru-(1.30)Sn/γ-Al<sub>2</sub>O<sub>3</sub> catalyst. (**Fig. S6**)
- 7) Photo images of reaction mixtures obtained after the second reaction run (**Fig. S7**).
- 8) ATR-IR spectra of recovered Ru-(1.30)Sn/γ-Al<sub>2</sub>O<sub>3</sub>(E) after the second reaction run (**Fig. S8**).
- 9) ICP analysis of typical Ru-(1.30)Sn/g-Al<sub>2</sub>O<sub>3</sub>(E) catalyst before and after catalytic reactions (Table S1.)

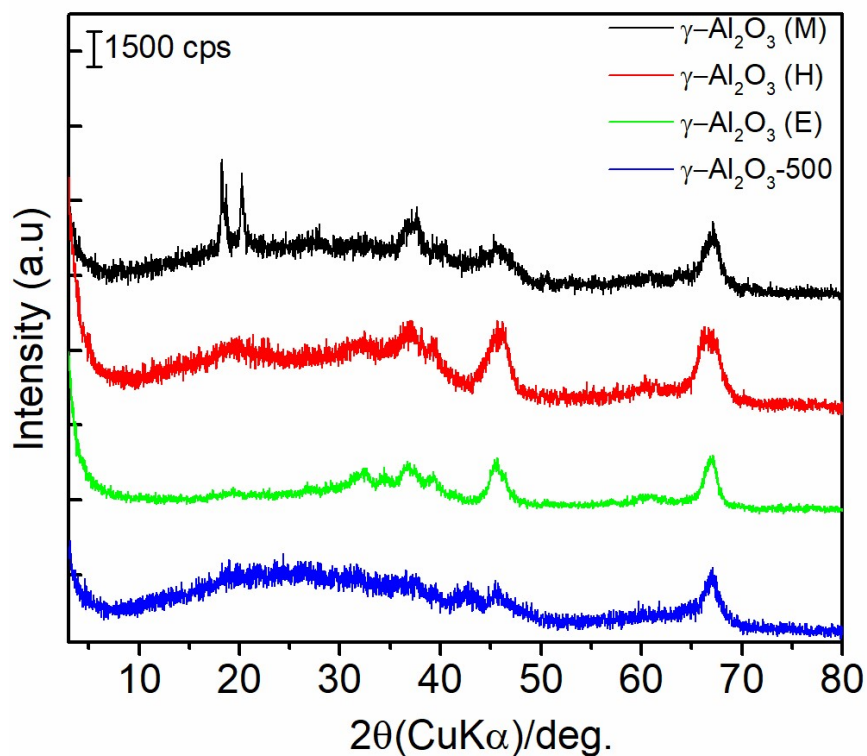


**Fig. S1** XRD patterns of the hydrargillite-derived  $\gamma$ - $\text{Al}_2\text{O}_3$ -500, and three types commercially available of Cariact- $\gamma$ - $\text{Al}_2\text{O}_3$ (E) (Evonik); ( $\gamma$ - $\text{Al}_2\text{O}_3$ (H)( HWNANO), and  $\gamma$ - $\text{Al}_2\text{O}_3$ (M) (Merck).

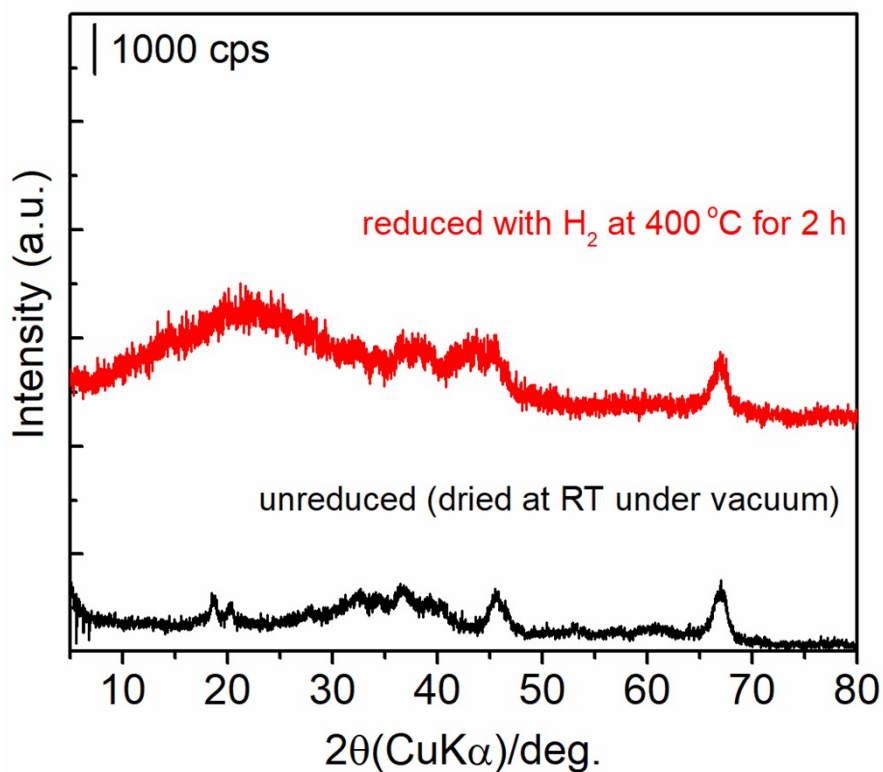


**Fig. S2** XRD patterns of unreduced (as-prepared) and reduced Ru-(1.30)Sn/ $\gamma$ - $\text{Al}_2\text{O}_3$ (E) samples.

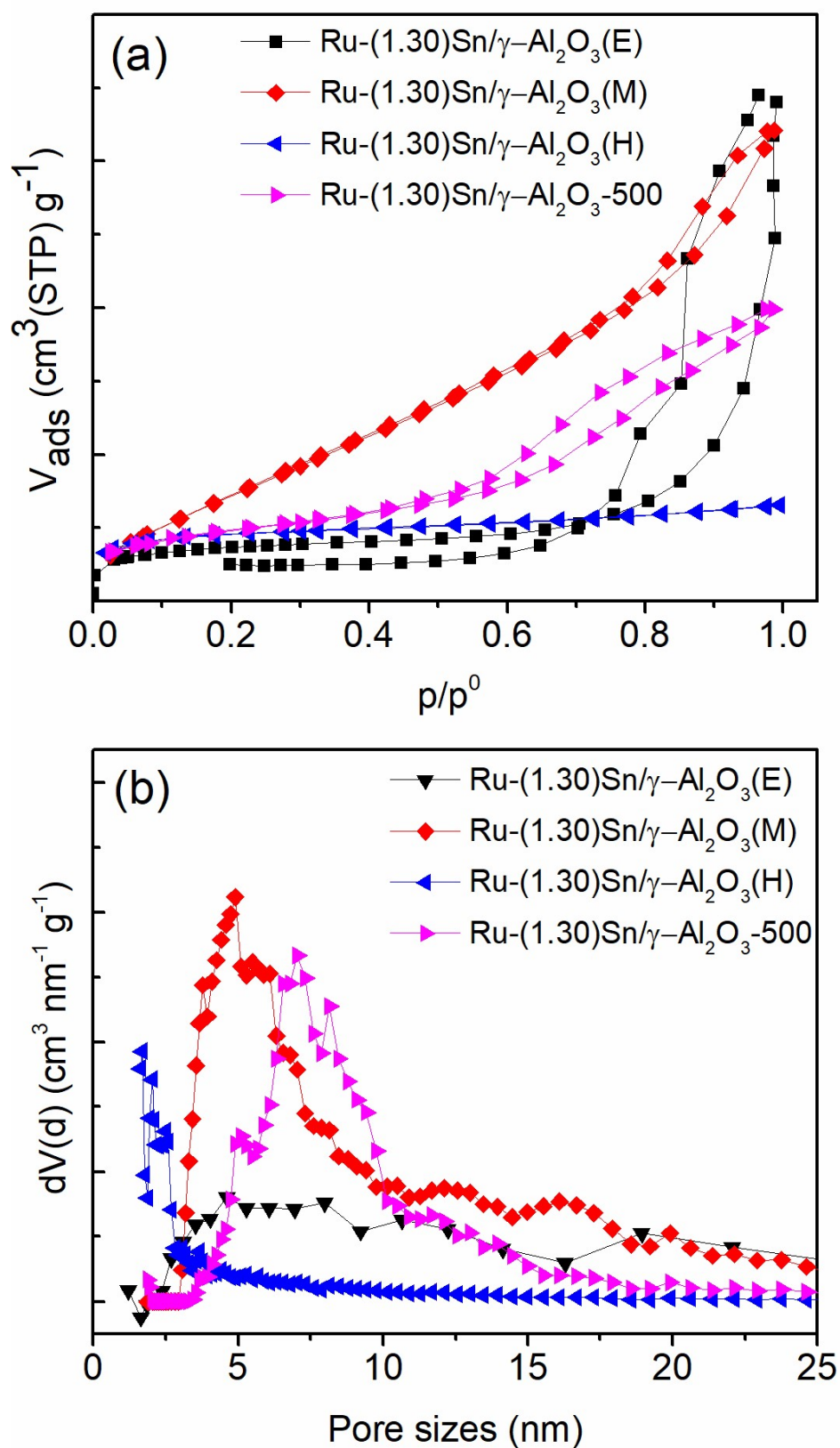


**Fig. S3** (a) N<sub>2</sub>-adsorption-desorption profiles and (b) pore sizes distribution determined by DFT method for four types of gamma-alumina-based supported Ru-(1.30)Sn catalysts after reduction with H<sub>2</sub> at 400 °C for 2 h.

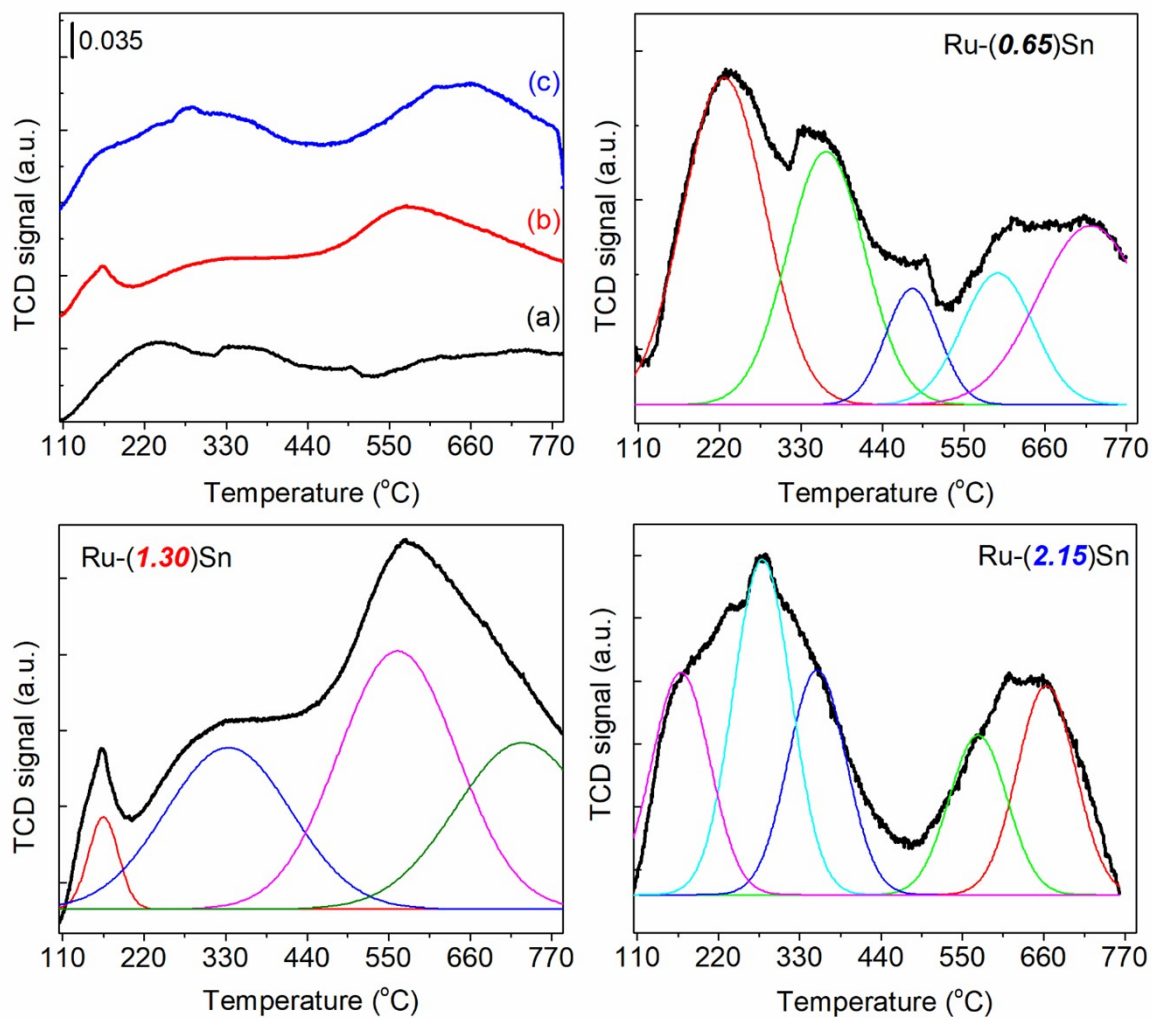


**Fig. S4** NH<sub>3</sub>-TPD profiles of Ru-(x)Sn/ $\gamma$ -Al<sub>2</sub>O<sub>3</sub>(E) and deconvoluted NH<sub>3</sub>-TPD spectra of Ru-(0.65)Sn/ $\gamma$ -Al<sub>2</sub>O<sub>3</sub>(E), Ru-(1.30)Sn/ $\gamma$ -Al<sub>2</sub>O<sub>3</sub>(E), and Ru-(2.15)Sn/ $\gamma$ -Al<sub>2</sub>O<sub>3</sub>(E) catalysts.

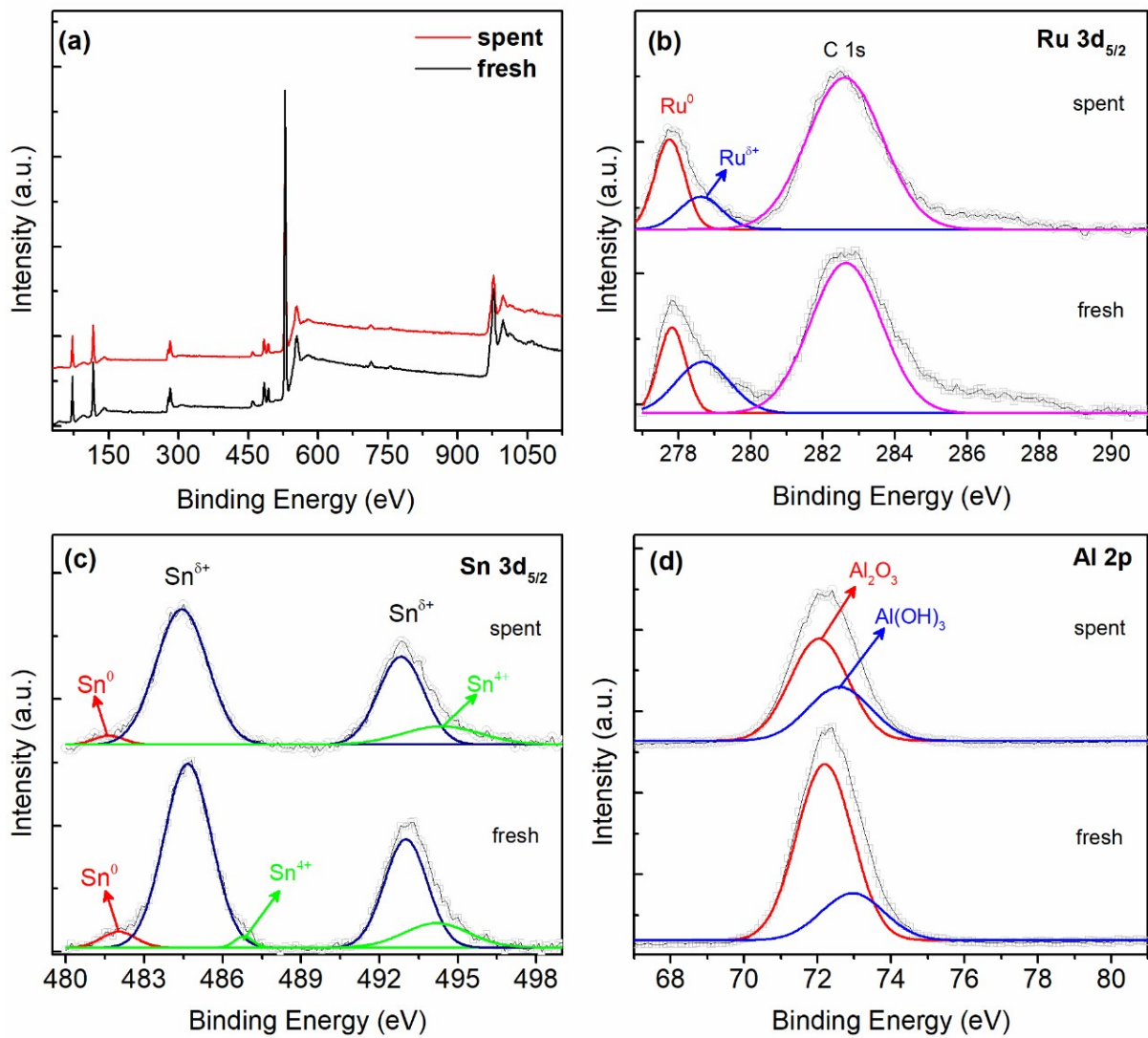


**Fig. S5** XPS spectra Al 2p for fresh and spent Ru-(1.30)Sn/g-Al<sub>2</sub>O<sub>3</sub>(E) samples.

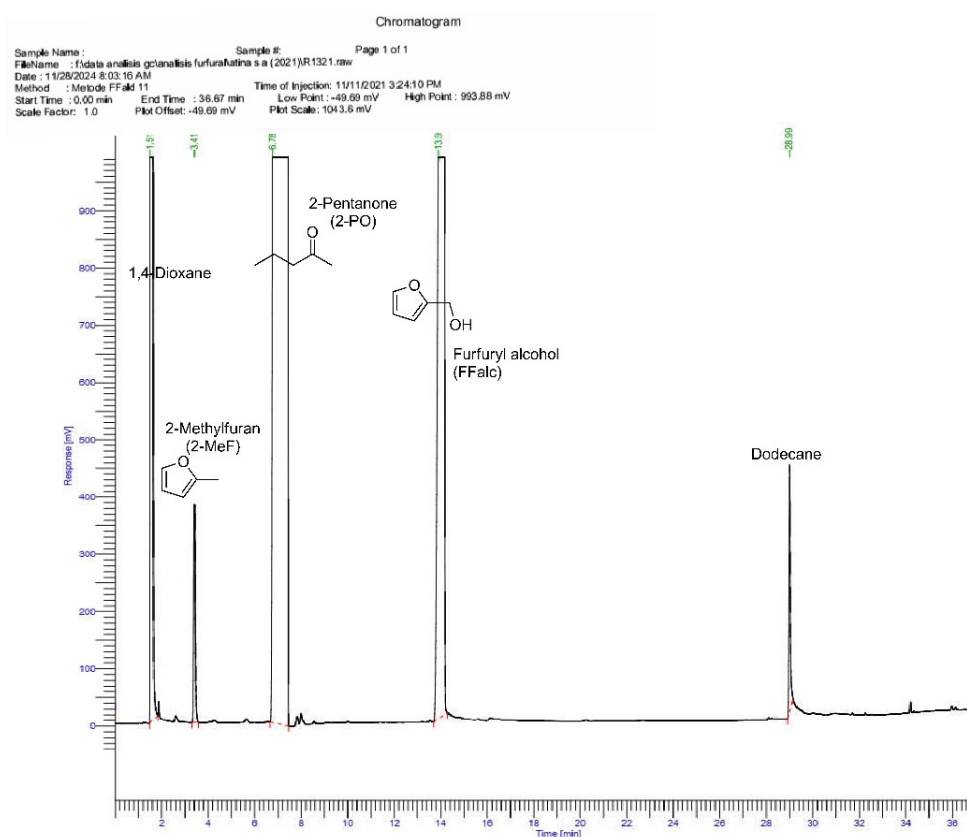


**Fig. S6** GC chart (chromatogram) of reaction mixture obtained from the reaction of FFald in 1,4-dioxane using the most effective Ru-(1.30)Sn/ $\gamma$ -Al<sub>2</sub>O<sub>3</sub> catalyst. Reaction conditions: catalyst, 50 mg; substrate (FFald), 2.0 mmol; solvent, 1,4-dioxane; 3.0-3.5 ml; initial H<sub>2</sub> pressure, 30 bar; 180 °C, 3 h.



**Fig. S7** Photo images of reaction mixtures obtained after the third reaction run using Ru-(1.30)Sn/ $\gamma$ -

Al<sub>2</sub>O<sub>3</sub> catalyst.

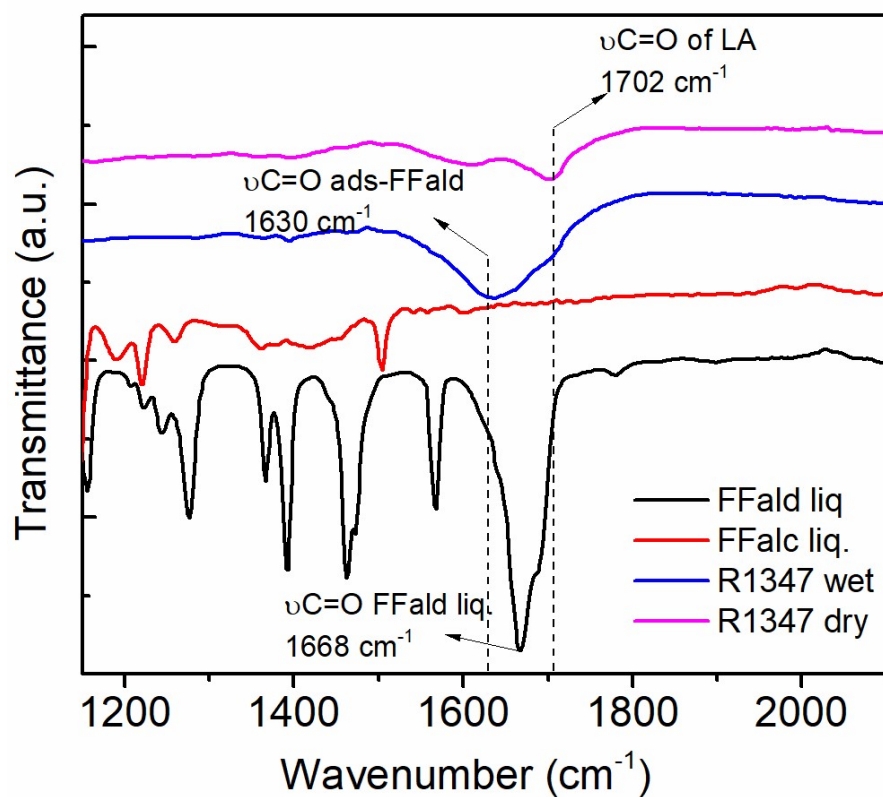


**Fig. S8** ATR-IR spectra of recovered Ru-(1.30)Sn/γ-Al<sub>2</sub>O<sub>3</sub>(E) after the second reaction run.

**Table S1.** ICP analysis of typical Ru-(1.30)Sn/g-Al<sub>2</sub>O<sub>3</sub> (E) catalyst before and after catalytic reactions

Entry	Catalyst	Bulk composition (mmol g <sup>-1</sup> )		
		Sn/Ru	Ru	Sn
1	Ru-(1.30)Sn/γ-Al <sub>2</sub> O <sub>3</sub> (E)	0.30	3.70	1.11
2 <sup>b</sup>	Ru-(1.30)Sn/γ-Al <sub>2</sub> O <sub>3</sub> (E) (recovered)	0.28	3.67	1.02

<sup>a</sup> Determined by ICP-AES.

<sup>b</sup> Recovered catalyst after reusability test.